

ECGadv: Generating Adversarial Electrocardiogram to Misguide Arrhythmia Classification System

Huangxun Chen^{1†}, Chenyu Huang^{1†}, Qianyi Huang¹, Qian Zhang¹

¹ The Hong Kong University of Science and Technology

hchenay@connect.ust.hk, chuangak@connect.ust.hk, qhuangaa@ust.hk, qianzh@cse.ust.hk

[†] Co-primary Authors

Abstract

Deep neural networks (DNNs)-powered Electrocardiogram (ECG) diagnosis systems emerge recently, and are expected to take over tedious examinations by cardiologists. However, their vulnerability to adversarial attacks still lack of comprehensive investigation. ECG recordings differ from images in the visualization, dynamic property and accessibility, thus, the existing image-targeted attack may not directly applicable. To fill this gap, this paper proposes ECGadv to explore the feasibility of adversarial attacks on arrhythmia classification system. We identify the main issues under two different deployment models (*i.e.*, cloud-based and local-based) and propose effective attack schemes respectively. Our results demonstrate the blind spots of DNN-powered diagnosis system under adversarial attacks, which facilitates future researches on countermeasures.

1 Introduction

Statistics [World Health Organization, 2018] has show that cardiovascular diseases are the worldwide leading health problem and the cause of death. In common clinical practice, ECG is an important tool to diagnose a wide spectrum of cardiac disorders. Traditionally, cardiologists review the ECG recordings to identify abnormalities, which heavily rely on their manual labor and medical expertise. In recent years, considerable approaches have been proposed for automatic ECG classification and diagnosis. The Deep Neural Networks (DNNs)-powered ones [Awni Y *et al.*, 2019] draws remarkable public attentions since they are capable of learning features directly from raw data without hand-engineered features.

Substantial algorithmic advances of DNNs boost the low-cost, accurate and early cardiac diagnosis to be widely available. Advanced DNNs-based ECG classification model can either work in smart devices (*e.g.*, Apple Watch 4) to provide real-time ECG monitoring (*i.e.*, local deployment model), or can be located on the cloud to facilitate tele-medicine for chronic patients at home or in rural communities (*i.e.*, cloud deployment model). Despite great potentials, DNNs' broad adoption has also aroused many public concerns on the algorithm reliability which people's health and lives rely on. Thus, there is an urgent need to investigate the possible breaches and vulnerability of DNNs-based diagnosis systems.

In the image domain, the state-of-the-art literatures have shown that an adversary can construct adversarial image by adding an almost imperceptible perturbations to the input image, which misleads DNNs to misclassify them into an incorrect class [Szegedy *et al.*, 2013; Goodfellow *et al.*, 2014; Carlini and Wagner, 2017]. However, the medical measurement (*e.g.*, ECG) domain still lacks investigation on the feasibility of adversarial attacks. ECG recordings are distinct from images in many aspects. In terms of visualization, ECGs are in time-amplitude format while images are in 2D color format. Each value in ECG represents the voltage of a sample point, and the data is visualized as line curve for examination. While each value in a image represents the grayscale or RGB value of a pixel, and it is visualized as the associated color for demonstration. In terms of dynamic property, medical data present more periodicity while images present more locality. In terms of accessibility, images are more accessible due to the booming of the Internet and social media, while ECGs are regarded as private data and have high acquisition costs for an adversary.

These differences require us to reconsider the adversarial attacks in the context of DNNs-based ECG classification system. For the cloud-based systems, the ECG recording may be often queried by cardiologists or patients themselves. Thus, we wonder whether it is possible for an adversary to corrupt an ECG example with sufficiently subtle perturbations to avoid arousing suspicion. Most image-targeted attacks utilized L_p norm to encourage visual imperceptibility of perturbations. They may not directly applicable on ECG because human has different perceptual sensitivity on colors and line curves. As shown in Fig. 1, when two data arraies are visualized as line curves, their differences are more prominent rather than those visualized as gray-scale images. Thus, this paper explores proper metrics to quantify perceptual similarity on line curves, and leverage them to generate unsuspecting adversarial instance for cloud-based ECG system attacks. For the local-based systems, an adversary can corrupt ECG via EMI signal injection [Kune *et al.*, 2013]. However, it is hard to obtain the current sampling point of the on-the-fly ECG recordings. The mismatch may make the perturbation intended for wave peak added onto wave valley. In addition, it is almost impossible to obtain every ECG recording especially when they are stored locally. Thus, this paper explicitly consider the possible mismatch in attack scheme to generate perturbations that are effective for the on-the-fly signals, and the perturbations obtained based on some instances can be applicable on other unseen ones as well.

In summary, the contributions of this paper are as follows:

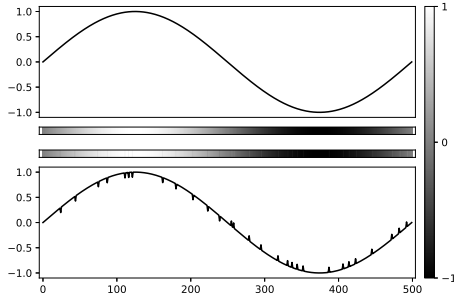


Figure 1: Perception test. There are two data arrays in the range of $[-1, 1]$, and the second one is obtained by adding a few perturbations with 0.1 amplitude to the first one. Both of them are visualized as line curves and gray-scale images.

- This paper takes the first step to investigate the adversarial attacks in DNNs-based ECG classification system. We identify the main issues under two different deployment models (*i.e.*, cloud-based and local-based) and propose effective attack schemes respectively.
- In attacks for the cloud deployment model, this paper propose a smoothness metric to quantify human perceptual distance on line curves, which captures the pattern similarity with computing efficiency (Section 4.1). The adversarial attacks using smoothness metric achieve 99.9% success rate. In addition, we conduct extensive human perceptual study on both ordinary people and cardiologists to evaluate the imperceptibility of adversarial ECG instances(Section 5.1).
- In attacks for the local deployment model, we model the sampling point uncertainty of the on-the-fly signals within the adversarial generation scheme (Section 4.2). The generated perturbation are shift-resistant to tamper the on-the-fly signals (99.55% success rate), and universal to attack on unseen examples (Section 5.2).

2 Background

In this section, we firstly introduce the targeted DNN model that we apply attack schemes on for evaluation, then we illustrate the threat models for DNNs-based ECG classification system.

2.1 Targeted DNN model

We apply our attack strategies to the DNN-based arrhythmia classification system [Rajpurkar *et al.*, 2017; Andreotti *et al.*, 2017; Awni Y *et al.*, 2019]. An arrhythmia is defined as any rhythm other than normal rhythm. Early and accurate detection of arrhythmia types is important in detecting heart diseases and choosing appropriate treatment for a patient. If the detection algorithm is mislead to classify an arrhythmia as a normal rhythm, the patient may miss the optimal treatment period, while if a normal rhythm is misclassified as an arrhythmia, the patient may accept unnecessary inspection and treatment, which results in the waste of medical resources. Thus, this paper aims to explore the blind spots of such system to facilitate future reseaches on countermeasures.

The original model [Rajpurkar *et al.*, 2017] adopts 34-layer Residual Networks (ResNet) [He *et al.*, 2016] to

classify 30s single lead ECG segment into 14 different classes. However, their dataset is not public. In the Physionet/Computing in Cardiology Challenge 2017 [Clifford *et al.*, 2017], [Andreotti *et al.*, 2017] reproduced the ResNet approach by [Rajpurkar *et al.*, 2017] on the dataset(denoted as PhyDB) and achieved good performance. Both their algorithm and model are available open-source.¹ The model architecture is shown in Figure 2. PhyDB dataset consist of 8,528 short single lead ECG segments labeled as 4 classes: normal rhythm(N), atrial fibrillation(A), other rhythm(O) and noise(\surd). Both atrial fibrillation and other rhythm indicates arrhythmia. Atrial fibrillation is the most prevalent cardiac arrhythmia and can occur in sustained or intermittent episodes. ‘‘Other rhythm’’ in the dataset refers to other arrhythmia except atrial fibrillation.

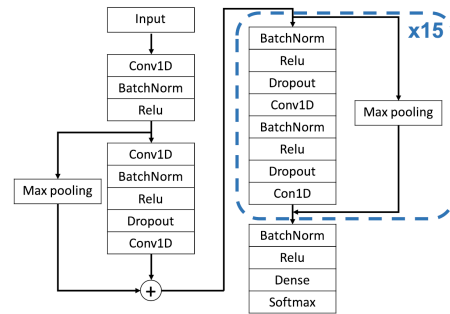


Figure 2: Architecture of Targeted Model.

2.2 Threat Models

As introduced above, DNN-based arrhythmia classification system can be deployed on the cloud or local devices.

In cloud deployment model, echocardiograms (ECGs) are measured in local using portable ECG patches like Life Signal LP1100² or household medical instruments like Heal Force ECG monitor³, and then uploaded to the cloud through the paired smartphone/PC. The ECG classification system on the cloud conducts analysis and handles data queries from both patients and cardiologists. The attacker may conduct middle-man attack to corrupt the data before uploading to the cloud. The corrupted data misleads the ECG classification system to give the incorrect diagnosis, and in the meanwhile, the data perturbations should be sufficiently subtle that they are either imperceptible to humans, or if perceptible, seems natural and not representative of an attack.

In local deployment model, ECGs are measured and analyzed in local device. A DNNs-based ECG classification model is compressed and stored in the local devices. The attacker may inject the perturbations to the on-the-fly ECG signals in real time to mislead the classifier. The attacker tries to maximize the success probability of attacks to disturb the normal operation of ECG monitoring devices.

3 Related Works

Here we review recent works on adversarial examples, and the existing arrhythmia classification systems.

¹<https://github.com/fernandoandreotti/cinc-challenge2>

²<https://lifesignals.com/products-services/>

³<http://www.healforce.com/en/index.php?ac=article&at=>

3.1 Adversarial Examples

In the state-of-the-art literature, considerable attack strategies have been proposed to generate adversarial examples.

Attacks can be classified into targeted and untargeted attack based on the adversarial goal. In targeted attack, the adversary modifies an input to mislead the target model to classify the perturbed input into a chosen class. While the adversary of untargeted attack aims to make the perturbed input to be misclassified to any class other than ground truth. In this paper, we only focus on the more powerful targeted attacks.

According to the accessibility to the target model, the existing attacks fall into two categories, white-box and black-box attack. In white-box manner, an adversary has complete access to a classifier [Szegedy *et al.*, 2013; Goodfellow *et al.*, 2014; Carlini and Wagner, 2017; Kurakin *et al.*, 2016], while in black-box manner, an adversary has zero knowledge about them [Papernot *et al.*, 2016; Moosavi-Dezfooli *et al.*, 2017; Liu *et al.*, 2016]. In this paper, we study the adversarial attacks in white-box setting. On one side, we would like to explore the upper bound of an adversary to better motivate defense methods. On the other side, prior works [Papernot *et al.*, 2016; Liu *et al.*, 2016] have shown the transferability of adversarial attacks, i.e, it is possible to train a substitute model given black-box access to a target model, and transfer the attacks to it by attacking the substitute one.

In the image domain, most existing works adopted L_p norm as approximations of human perceptual distance to constrain the distortion. However, for medical data in time series format, people focus more on the overall pattern/shape, which requires other distance metric to quantify (see Section 4.1 for more details).

Recent works [Kurakin *et al.*, 2016; Athalye and Sutskever, 2017; Chen *et al.*, 2018] have explored the robustness of the adversarial examples in physical world, where the input images could not be precisely controlled, and may change under different viewpoints, lighting and camera noise. Our attack strategy on local deployment model is inspired by [Athalye and Sutskever, 2017; Brown *et al.*, 2017]. Different from images, we deal with sampling point uncertainty of the on-the-fly signals.

3.2 Arrhythmia Classification System

Considerable efforts have been made on automated arrhythmia classification systems to take over tedious examinations by cardiologists. The major challenges are lack of feature standardization, intra-features variability and inter-patients variability [Jambukia *et al.*, 2015]. Deep learning methods show great potentials due to their ability to automatically learn features through multiple levels of abstraction, which frees the system from the dependence on hand-engineered features. Recent works [Kiranyaz *et al.*, 2016; Al Rahhal *et al.*, 2016; Awni Y *et al.*, 2019] started applying DNN models on ECG signals for arrhythmia classification and achieved good performance. For any system in healthcare field, it is crucial to defend the possible attacks since people’s lives rely heavily on the system reliability. Prior work [Kune *et al.*, 2013] has launched attacks to pollute the measurement of cardiac devices by a low-power emission of chosen electromagnetic waveforms. The adversarial attacks studied in this paper and the injection attacks in [Kune *et al.*, 2013] complement each other. The injection attack can inject the carefully-crafted perturbation generated

by adversarial attacks to perform targeted attacks to mislead the arrhythmia classification system on cardiac devices.

4 Technical Approach

In this section, we illustrate our attack strategies for cloud and local deployment model respectively.

4.1 Attack Strategy for Cloud Deployment Model

Problem Formulation

Given a m-class classifier, $g : \mathcal{X} \rightarrow \mathcal{Y}$ that accept an input $x \in \mathcal{X}$ and produces an output $y \in \mathcal{Y}$. The output vector y , treated as probability distribution, satisfies $0 \leq y_i \leq 1$ and $\sum_{i=1}^m y_i = 1$. The classifier assigns the label $C(x) = \text{argmax}_i g(x)_i$ to the input x . Let $C^*(x)$ be the correct label of x . Given a valid input x and a target class $t \neq C^*(x)$, an adversary aims to generate adversarial examples x_{adv} so that the classifier predicts $g(x_{adv}) = t$ (i.e. successful attack), and x_{adv} and x are close based on the similarity metric (i.e. visual imperceptibility). it can be modeled as a constrained minimization problem as prior works [Szegedy *et al.*, 2013]:

$$\begin{aligned} & \text{minimize } \mathcal{D}(x, x_{adv}) \\ & \text{such that } C(x_{adv}) = t \end{aligned} \quad (1)$$

where \mathcal{D} is some similarity metric. It is worth mentioning that there is no box constraints for time-series measurement. It is equivalent to solve [Carlini and Wagner, 2017]:

$$\text{minimize } \mathcal{D}(x, x_{adv}) + c \cdot f_{g,t}(x_{adv}) \quad (2)$$

where $f_{g,t}$ is an objective function mapping the input to a positive number, which satisfies $f_{g,t}(x_{adv}) \leq 0$ if and only if $C(x_{adv}) = t$. One common objective function is cross-entropy. We adopt the one as in [Carlini and Wagner, 2017].

$$f_{g,t}(x_{adv}) = (\max_{i \neq t} (Z(x_{adv})_i) - Z(x_{adv})_t)^+ \quad (3)$$

where $Z(x) = z$ is logits, i.e., the output of all layers except the softmax. $(e)^+$ is short-hand for $\max(e, 0)$.

Similarity Metrics

To generate adversarial examples, we require a distance metric to quantify perceptual similarity to encourage visual imperceptibility. The widely-adopted distance metrics in the literature are L_p norms $\|x - x'\|_p$, where the p-norm $\|\cdot\|_p$ is defined as

$$\|v\|_p = \left(\sum_{i=1}^n |v_i|^p \right)^{\frac{1}{p}} \quad (4)$$

L_p norms focus on the change of each pixel values. However, human perception on line curves focus more on the overall pattern/shape. Studies in [Eichmann and Zraggen, 2015; Gogolou *et al.*, 2018] show that given a group of line curves for similarity assessment, pattern-focused distance metrics like Dynamic time warping (DTW) produce rankings that are closer to the human-annotated rankings than other metrics like Euclidean distance. DTW is widely-adopted to quantify the similarity of time series. However, the non-differentiability and non-parallelism make it ill-suited for adversarial attacks. Recent work [Cuturi and Blondel, 2017] proposed a differentiable DTW variant, Soft-DTW. However, Soft-DTW doesn’t change the essence of DTW – a standard dynamic programming problem. The value and gradient of

Soft-DTW would be computed with quadratic time, and it is hard to leverage parallel computing of GPU to speed up.

To capture the pattern similarity with computation efficiency, we adopt the following metric, denoted as *smoothness* as our similarity metric. Given $\delta = x' - x$ and $\text{var}(\cdot)$ refers to variance calculation:

$$\begin{aligned} \text{diff}(\delta) &= \delta_i - \delta_{i-1}, i = 2, \dots, n \\ d_{\text{smooth}}(\delta) &= \text{var}(\text{diff}(\delta)) \end{aligned} \quad (5)$$

Smoothness metric d_{smooth} quantifies the smoothness of perturbation(δ) by measuring the variation of the difference between neighbouring points of perturbation. The smaller the variation, the smoother the perturbation. A smoother perturbation δ means that the adversarial instances x' are more likely to preserve similar pattern as the original instance x . In the extreme case where $d_{\text{smooth}} = 0$, δ should be a constant and $x' = x + \text{constant}$, i.e., the adversarial instances x' has the same pattern as the original instance x . Besides, smoothness metric can be computed with linear time and can be accelerated by parallel computing as L_2 norm, which is favorable in adversarial attacks.

4.2 Attack Strategy for Local Deployment Model

Problem Formulation

Given the same m-class classifier, $g : \mathcal{X} \rightarrow \mathcal{Y}$ as in cloud deployment model, there exists uncertainty of current sample point of the on-the-fly signal in local deployment model. Inspired by *Expectation Over Transformation(EOT)* [Athalye and Sutskever, 2017], we regard such uncertainty as a shifting transformation of the original measurement and explicitly consider the transformation within the optimization procedure. Given a distance function $\mathcal{D}(\cdot, \cdot)$ and a chosen distribution T of transformation function t , we aim to constrain the expected effective distance between the adversarial and original inputs:

$$\gamma = \mathbb{E}_{t \in T}[\mathcal{D}(t(x_{adv}), t(x))] \quad (6)$$

Thus, the adversarial attacks can be modeled as follows:

$$\underset{x_{adv}}{\text{argmax}} \mathbb{E}_{t \in T}[\log Z(t(x_{adv}))_t] \quad (7)$$

Here we add a constraint $\mathcal{D}(t(x_{adv}), t(x)) < \epsilon$, which forces the adversarial examples to be within certain distance constraint of the original one. However, ϵ is large enough that x_{adv} can have a large probability that attacks successfully in most time positions. Moreover, since the ECG signals of the same class from different people are quite similar to each other, sufficiently large ϵ can provide the universality of adversarial sample, i.e., a x_{adv} can take effect on those ECG signals with the same class as the training sample x .

We maximize the objective using Adam [Kingma and Ba, 2014] optimizer, and approximate the gradient of the expected value through sampling transformations independently at each gradient decent step.

Perturbation Window Size

Since we attack the device with on-the-fly signals, we hope such perturbation may not attract too much attentions from the victim. Thus we introduce a new parameter, the length of the perturbation w_d , which is set by the attacker and fixed during the optimization. w_d gives the system flexibility to control the added perturbation. The intuition of this parameter is that the smaller w_d , the less chance that the victim perceives the attack, because it takes less time to generate and launch such

attack. On the other hand, the larger w_d , the generated x_{adv} is more universal since it can influence more sample points.

5 Experimental Results

In this section, we evaluate our attacks for cloud deployment model and local deployment model respectively.

5.1 Evaluation for cloud deployment model

Experiment Setup

We implement our attack strategy for cloud deployment model under the framework of CleverHans [Papernot *et al.*, 2018]. We adopt the Adam optimizer [Kingma and Ba, 2014] with 0.005 learning rate to search adversarial examples. We compare the performance of three similarity metrics on adversarial examples generation, given $\delta = x_{adv} - x$

- $d_{l2}(\delta) = \|\delta\|_2^2$
- $d_{\text{smooth}}(\delta)$ (Equation 5)
- $d_{\text{smooth},l2}(\delta) = d_{\text{smooth}}(\delta) + k \cdot d_{l2}(\delta)$, $k = 0.01$

All metrics are evaluated under the same optimization scheme with the same hyper-parameters. Notice that the target model is not accurate on all ECG segments in PhyDB dataset. Therefore, we only generate adversarial examples for those segments correctly classified by the model. The profile for the attack dataset is shown in Table 1. Here, ‘‘A, N, O, \surd ’’ denote normal rhythm, atrial fibrillation(AF), other rhythm and noisy signal respectively in the following evaluation. The sampling rate of the ECG segment is 300Hz, i.e., the length of a 30s ECG segment is 9000. The input vector of the target model in Figure 2 is 9000.

Table 1: Data profile for the attack dataset

Type	Number	Time length (s)	
		mean	std
Normal rhythm(N)	3886	32.85	9.70
Atrial Fibrillation(A)	447	32.25	11.98
Other rhythm(O)	1488	35.46	11.56
Noisy signal(\surd)	260	24.02	10.42

Success Rate of Targeted Attacks

We select first 360 segments of class N, first 360 of class A, first 360 of class O and first 220 of class \surd in attack dataset to evaluate the success rate of targeted attacks. For each ECG segment, we conduct three targeted attacks to other classes one by one. Thus, we have 12 source-target pairs given 4 classes. The attack results are shown in Table 2.

With all three similarity metrics, the generated adversarial instances achieve quite high attack success rates. d_{l2} fail on a few instances of some source-target pairs, such as ‘‘O \rightarrow A’’, ‘‘A \rightarrow N’’, ‘‘O \rightarrow N’’ and ‘‘ $\surd \rightarrow$ N’’. d_{smooth} case achieves almost 100% success rate and $d_{\text{smooth},l2}$ achieves 100% success rate. A sample of generated adversarial ECG signals are shown in Fig. 3. Due to the limited space, we only show a case where an original atrial fibrillation ECG is misclassified to normal rhythm. It is noticed that the one generated with d_{l2} metric looks more suspicious due to lots of small spikes, while the d_{smooth} one preserves more similar pattern as the original one. The property of the $d_{\text{smooth},l2}$ one falls in between the above two as expected.

Table 2: Success rates of targeted attacks (cloud-based model)

	d_{l_2}				d_{smooth}				d_{smooth,l_2}			
	A	N	O	\sim	A	N	O	\sim	A	N	O	\sim
A	/	97.22%	100%	100%	/	100%	100%	100%	/	100.0%	100.0%	100.0%
N	100%	/	100%	100%	100%	/	100%	100%	100%	/	100%	100%
O	99.44%	95.0%	/	100%	99.72%	100%	/	100%	100%	100%	/	100%
\sim	100%	99.55%	100%	/	100%	100%	100%	/	100%	100%	100%	/

Human Perceptual Study

We conduct extensive human perceptual study on both ordinary people and cardiologists to evaluate the imperceptibility of adversarial ECG instances. The ordinary human participants are recruited from Amazon Mechanical Turk (AMT), who don't have relevant medical expertise. Thus, they are only required to compare the adversarial examples generated using different similarity metrics and choose the one closer to the original ECG. For each similarity metric, we generate 600 adversarial examples from PhyDB dataset (each source-target pair accounts for 50 examples). In the study, the participants are asked to observe an original example and its two adversarial ones generated using two different similarity metrics. Then they need to choose the one from two adversarial examples that is closer to the original one. The perceptual study consist of three parts, (i) d_{smooth} versus d_{l_2} , (ii) d_{smooth,l_2} versus d_{l_2} , (iii) d_{smooth} versus d_{smooth,l_2} . To avoid labeling bias, we allow each user to conduct at most 60 trials. For each tuple of an original example and its two adversarial examples, we collect 5 annotations from different participants. In total, we collected 9000 annotations from 57 AMT users. The study results are shown in Table 3, where "triumph" denotes the metric get 4 or 5 votes out of all 5 annotations, and "win" denotes a metric gets 3 votes out of 5, *i.e.*, a narrow victory.

Table 3: Human perceptual study (AMT participants)

(i)	d_{smooth} win(%)			d_{l_2} win(%)		
	triumph	win	total	triumph	win	total
	58.67	22.67	81.34	10	8.66	18.66
(ii)	d_{smooth,l_2} win(%)			d_{l_2} win(%)		
	triumph	win	total	triumph	win	total
	65.5	18.5	84	7.83	8.17	16
(iii)	d_{smooth} win(%)			d_{smooth,l_2} win(%)		
	triumph	win	total	triumph	win	total
	31.83	27.83	59.67	15.83	24.5	40.33

Compared with d_{l_2} -generated example, d_{smooth} -generated ones are voted to be closer to the original in 81.34% of the trials. In comparison between d_{l_2} and d_{smooth,l_2} , the latter is voted as the winner in 84% of the trials. This indicates that the smoothness metric encourages generated adversarial examples preserve similar pattern as the original one, so that they are more likely to be imperceptible. In comparison between d_{smooth} and d_{smooth,l_2} , d_{smooth} get a little more votes (59.67%) than d_{smooth,l_2} , which further validates that smoothness metric is more suitable to qualify human similarity perception on line curves than L_2 norm.

Besides participants on AMT, we also invite three cardiologists to evaluate whether added perturbations arouse their

suspicion and influence their medical judge. The cardiologists are asked to classify the given ECG and its adversarial counterparts into 4 classes (A, N, O, \sim) based on their medical expertise. As illustrated in Section 2.1, it is significant to distinguish normal rhythms and abnormal rhythms. Thus, we focus on the cases of "N \rightarrow A", "N \rightarrow O", "A \rightarrow N", "O \rightarrow N", which misclassify a normal rhythm to an arrhythmia or vice versa. For above 4 source-target pairs, we randomly select 3 type N, another 3 type N, 3 type A and 3 type O, then we conduct corresponding targeted attacks with different similarity metrics to generate adversarial examples. Thus, we have 48 adversarial examples in total and shuffle them randomly. For every example, we collect annotations from all three cardiologists. The study results are shown in Table 4.

Table 4: Human Perceptual Study (Cardiologists)

Idx	Original	d_{l_2}	d_{smooth}	d_{smooth,l_2}
1	100%	100%	100%	100%
2	91.7%	100%	100%	100%
3	100%	100%	100%	100%

Every row refers to one cardiologist. The first column denotes the percentage of the cardiologist's annotations which are the same as the labels in original PhyDB dataset. Only one cardiologist annotates an type A instance as type O. The last three column shows the percentage of adversarial examples which are annotated the same as their original counterparts. High percentage means that added perturbations don't arouse their suspicion and influence their medical judge. The results show that in all cases, cardiologists give the same annotations to adversarial examples as their original counterparts. The possible reason is that most perturbations generally occur on the wave valley, but the cardiologists give annotations based on the peak-to-peak intervals. Thus, the cardiologists regard the subtle perturbations as instrument noise.

5.2 Evaluation for local deployment model

Success Rate of Targeted Attacks

We implement our attack strategy for local deployment model under the framework of CleverHans [Papernot *et al.*, 2018]. Among 12 source-target pairs, we randomly choose 10 samples of each pair to generate adversarial perturbations by applying the attack strategy in Section 4.2. It is worth mentioning that we generate one perturbation from one samples. Thus, we have 10 perturbations from 10 samples. Then we apply the above perturbations to random-chosen 100 samples of the corresponding source class to see whether the adversarial examples could mislead the classifier universally. To mimic the uncertainty of the current sample point of the on-the-fly signals, we generate the perturbation with full length which means w_d is equal to 9000. Then we randomly shift perturbations and add it to the original signals. In this evalu-

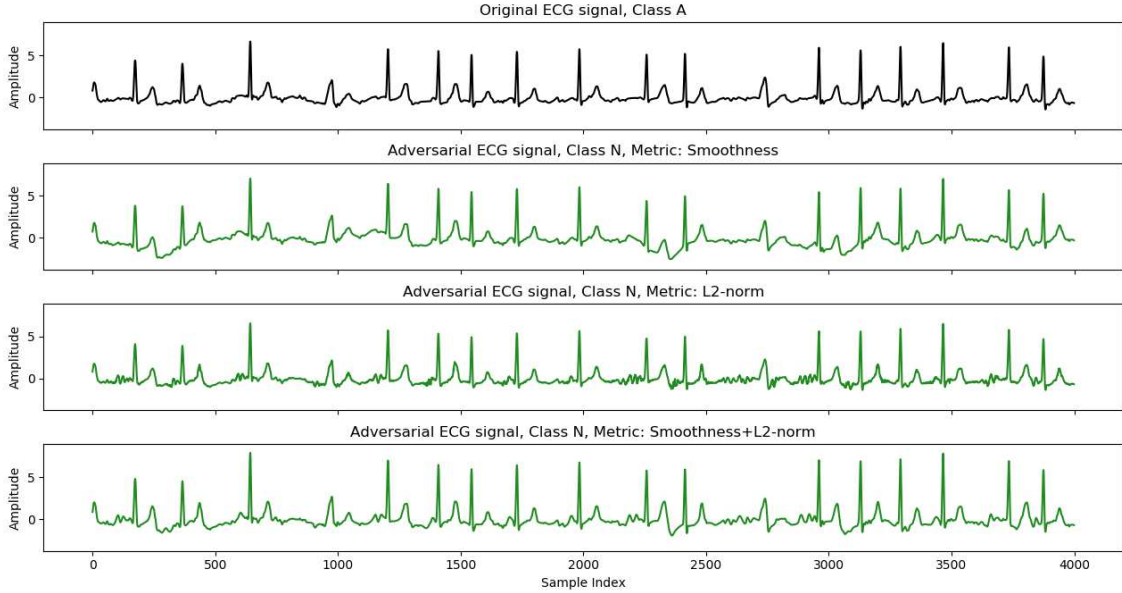


Figure 3: A sample of generated adversarial ECG signal.

ation, we randomly shift the perturbations 200 times to test. The average success rates are shown in Table 5. Our attack strategy achieves pretty high success rates, which indicates that the generated perturbation is both shifting-resistant and universal.

Table 5: Success rates of targeted attacks (local model)

	A	N	O	\sim
A	/	99.87%	99.96%	99.97%
N	100%	/	100%	99.97%
O	100%	99.46%	/	100%
\sim	98.66%	98.23%	98.48%	/

Impact of Window Size

In this section, we evaluate the accuracy under different window size w_d .

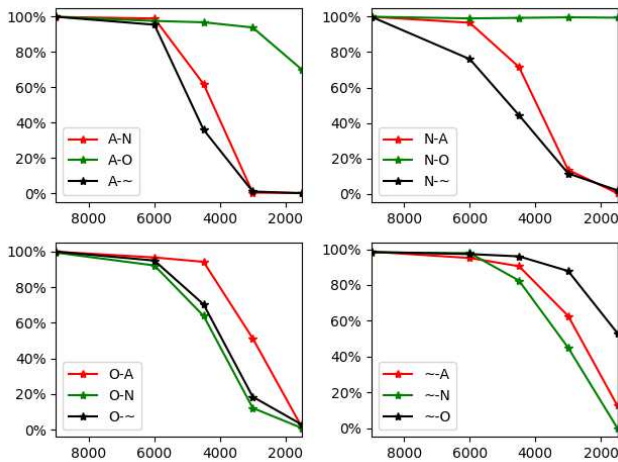


Figure 4: Success attack rates with different window size.

As we mentioned before, the smaller window size, the

lower chance that the attacker can be detected. Thus, we generate perturbations at different window size of 9000, 6000, 4500, 3000 and 1500. For each window size, we generate adversarial examples under the same condition as the previous section – randomly 10 samples for 12 source-target pairs. Then we shift the perturbation in random and add it to samples from origin source pair. The results are shown in Figure 4. We can see that in most cases the success rates decrease a lot when the window size increase. However, they slowly decrease and even remain almost unchanged under the cases of “A \rightarrow O”, “N \rightarrow O” and “ \sim \rightarrow O”. All these cases are from one class to class O. This is mainly because the class O covers many different situations. In the sub-figures, we find that except class O, the success rate decrease slower when target class is A than others. This is because if the part of the ECG signal is A, then the whole ECG segment can be classified as A.

6 Conclusion

This paper proposes ECGadv to generate adversarial ECG examples to misguide both cloud-based and local-based arrhythmia classification system. We identify the main issues under two different deployment models and propose effective attack schemes respectively. In attacks for the cloud deployment model, this paper propose a smoothness metric to encourage visual imperceptibility. Extensive human perceptual study on both ordinary people and cardiologists validate the visual imperceptibility of adversarial ECG instances. In attacks for the local deployment model, we model the sampling point uncertainty of the on-the-fly signals within the adversarial generation scheme. The generated perturbation are shift-resistant to tamper the on-the-fly signals with high success rate, and universal to attack on unseen examples. This paper reveals the blind spots of DNN-powered ECG classification system to adversarial attacks, which facilitates future research on countermeasures.

References

- [Al Rahhal *et al.*, 2016] Mohamad M Al Rahhal, Yakoub Bazi, Haikel AlHichri, Naif Alajlan, Farid Melgani, and Ronald R Yager. Deep learning approach for active classification of electrocardiogram signals. *Information Sciences*, 345:340–354, 2016.
- [Andreotti *et al.*, 2017] Fernando Andreotti, Oliver Carr, Marco AF Pimentel, Adam Mahdi, and Maarten De Vos. Comparing feature-based classifiers and convolutional neural networks to detect arrhythmia from short segments of ecg. *Computing*, 44:1, 2017.
- [Athalye and Sutskever, 2017] Anish Athalye and Ilya Sutskever. Synthesizing robust adversarial examples. *arXiv preprint arXiv:1707.07397*, 2017.
- [Awni Y *et al.*, 2019] Hannun Awni Y, Rajpurkar Pranavm, Haghpanahi Masoumeh, Tison Geoffrey H, Bourn Codie, Turakhia Mintu P, and Ng Andrew Y. Cardiologist-level arrhythmia detection and classification in ambulatory electrocardiograms using a deep neural network. *Nature Medicine*, pages volume 25, 65–69, 2019.
- [Brown *et al.*, 2017] Tom B Brown, Dandelion Mané, Aurko Roy, Martín Abadi, and Justin Gilmer. Adversarial patch. *arXiv preprint arXiv:1712.09665*, 2017.
- [Carlini and Wagner, 2017] Nicholas Carlini and David Wagner. Towards evaluating the robustness of neural networks. In *2017 IEEE Symposium on Security and Privacy (SP)*, pages 39–57. IEEE, 2017.
- [Chen *et al.*, 2018] Shang-Tse Chen, Cory Cornelius, Jason Martin, and Duen Horng Chau. Robust physical adversarial attack on faster r-cnn object detector. *arXiv preprint arXiv:1804.05810*, 2018.
- [Clifford *et al.*, 2017] Gari D Clifford, Chengyu Liu, Benjamin Moody, Li-wei H Lehman, Ikaro Silva, Qiao Li, AE Johnson, and Roger G Mark. Af classification from a short single lead ecg recording: The physionet computing in cardiology challenge 2017. *Proceedings of Computing in Cardiology*, 44:1, 2017.
- [Cuturi and Blondel, 2017] Marco Cuturi and Mathieu Blondel. Soft-dtw: a differentiable loss function for time-series. *arXiv preprint arXiv:1703.01541*, 2017.
- [Eichmann and Zraggen, 2015] Philipp Eichmann and Emanuel Zraggen. Evaluating subjective accuracy in time series pattern-matching using human-annotated rankings. In *Proceedings of the 20th International Conference on Intelligent User Interfaces*, pages 28–37. ACM, 2015.
- [Gogolou *et al.*, 2018] Anna Gogolou, Theophanis Tsandilas, Themis Palpanas, and Anastasia Bezerianos. Comparing similarity perception in time series visualizations. *IEEE transactions on visualization and computer graphics*, 2018.
- [Goodfellow *et al.*, 2014] Ian J Goodfellow, Jonathon Shlens, and Christian Szegedy. Explaining and harnessing adversarial examples. *arXiv preprint arXiv:1412.6572*, 2014.
- [He *et al.*, 2016] Kaiming He, Xiangyu Zhang, Shaoqing Ren, and Jian Sun. Deep residual learning for image recognition. In *Proceedings of the IEEE conference on computer vision and pattern recognition*, pages 770–778, 2016.
- [Jambukia *et al.*, 2015] Shweta H Jambukia, Vipul K Dabhi, and Harshadkumar B Prajapati. Classification of ecg signals using machine learning techniques: A survey. In *Computer Engineering and Applications (ICACEA), 2015 International Conference on Advances in*, pages 714–721. IEEE, 2015.
- [Kingma and Ba, 2014] Diederik P Kingma and Jimmy Ba. Adam: A method for stochastic optimization. *arXiv preprint arXiv:1412.6980*, 2014.
- [Kiranyaz *et al.*, 2016] Serkan Kiranyaz, Turker Ince, and Moncef Gabbouj. Real-time patient-specific ecg classification by 1-d convolutional neural networks. *IEEE Transactions on Biomedical Engineering*, 63(3):664–675, 2016.
- [Kune *et al.*, 2013] Denis Foo Kune, John Backes, Shane S Clark, Daniel Kramer, Matthew Reynolds, Kevin Fu, Yongdae Kim, and Wenyuan Xu. Ghost talk: Mitigating emi signal injection attacks against analog sensors. In *Security and Privacy (SP), 2013 IEEE Symposium on*, pages 145–159. IEEE, 2013.
- [Kurakin *et al.*, 2016] Alexey Kurakin, Ian Goodfellow, and Samy Bengio. Adversarial examples in the physical world. *arXiv preprint arXiv:1607.02533*, 2016.
- [Liu *et al.*, 2016] Yanpei Liu, Xinyun Chen, Chang Liu, and Dawn Song. Delving into transferable adversarial examples and black-box attacks. *arXiv preprint arXiv:1611.02770*, 2016.
- [Moosavi-Dezfooli *et al.*, 2017] Seyed-Mohsen Moosavi-Dezfooli, Alhussein Fawzi, Omar Fawzi, and Pascal Frossard. Universal adversarial perturbations. *arXiv preprint*, 2017.
- [Papernot *et al.*, 2016] Nicolas Papernot, Patrick McDaniel, and Ian Goodfellow. Transferability in machine learning: from phenomena to black-box attacks using adversarial samples. *arXiv preprint arXiv:1605.07277*, 2016.
- [Papernot *et al.*, 2018] Nicolas Papernot, Fartash Faghri, Nicholas Carlini, Ian Goodfellow, Reuben Feinman, Alexey Kurakin, Cihang Xie, Yash Sharma, Tom Brown, Aurko Roy, Alexander Matyasko, Vahid Behzadan, Karen Hambardzumyan, Zhishuai Zhang, Yi-Lin Juang, Zhi Li, Ryan Sheatsley, Abhibhav Garg, Jonathan Uesato, Willi Gierke, Yinpeng Dong, David Berthelot, Paul Hendricks, Jonas Rauber, and Rujun Long. Technical report on the cleverhans v2.1.0 adversarial examples library. *arXiv preprint arXiv:1610.00768*, 2018.
- [Rajpurkar *et al.*, 2017] Pranav Rajpurkar, Awni Y Hannun, Masoumeh Haghpanahi, Codie Bourn, and Andrew Y Ng. Cardiologist-level arrhythmia detection with convolutional neural networks. *arXiv preprint arXiv:1707.01836*, 2017.
- [Szegedy *et al.*, 2013] Christian Szegedy, Wojciech Zaremba, Ilya Sutskever, Joan Bruna, Dumitru Erhan, Ian Goodfellow, and Rob Fergus. Intriguing properties of neural networks. *arXiv preprint arXiv:1312.6199*, 2013.
- [World Health Organization, 2018] World Health Organization. Cardiovascular disease is the leading global killer. https://www.who.int/cardiovascular_diseases/en/, 2018.